Experimental study of diffusive cooling of electrons in a pulsed inductively coupled plasma

Antonio Maresca, Konstantin Orlov, and Uwe Kortshagen
High Temperature and Plasma Laboratory, Department of Mechanical Engineering, University of Minnesota-Twin Cities, 111 Church Street Southeast, Minneapolis, Minnesota 55455
(Received 31 December 2001; published 2 May 2002)

Langmuir probe measurements of the temporal behavior of the electron distribution function in a low-pressure inductive discharge are presented. The structure of the measured distribution functions suggests that the loss of high energetic electrons to the wall of the discharge chamber is the main energy loss mechanism. Electron-heavy-particle collisions play only a secondary role for the energy loss. The rapid loss of energetic electrons—while low energy electrons remain confined in the space charge potential field—leads to a fast cooling of the electron distribution function. We also present a simple model to describe the evolution of the mean kinetic energy and plasma potential on the basis of a distribution function that is cutoff at energies above the potential electron energy at the wall.

DOI: 10.1103/PhysRevE.65.056405 PACS number(s): 52.80.Pi, 52.70.Ds, 51.10.+y

I. INTRODUCTION

Pulsed power plasmas have attracted attention due to their added control of the plasma process through variation of the pulse duration, the duty cycle, or the pulse shape. Several advantages of pulsed plasmas have been demonstrated such as improved etch selectivity [1,2], the reduction of charge accumulation on the substrate [2], improved quality of deposited films [3], or the reduction of particle contamination [4].

One main feature of pulsed plasmas is that they make available a spectrum of electron mean kinetic energies. (Note that since the electron distribution function usually deviates from a Maxwellian distribution it is more correct, though cumbersome, to talk about the electron mean kinetic energy instead of the electron temperature.) The electron mean energy increases rapidly during the breakdown phase and often shows an overshoot before it reaches a steady state value. In the afterglow the mean energy relaxes with a much faster rate than the electron density [5]. Due to the nonlinear dependence of most plasma chemical reactions on the electron energy, the pulse frequency and duty cycle can creatively be used to adjust the plasma chemistry.

Several mechanisms can be responsible for the relaxation of the electron distribution function (EDF) in the afterglow of pulsed plasmas. It is widely known that electron-atom collisions are one main mechanism leading to electron energy relaxation [6–11] in time-varying electric fields. However, in low-pressure discharges operating at pressures of a few Pa collisions are rare and energy relaxation may proceed through a different channel.

Already in 1954 Biondi [12] identified the loss of electrons to the walls of the discharge container as the dominant electron cooling mechanism in his plasma and named this effect ''diffusive cooling.'' Biondi clearly outlined the physical scenario leading to this effect (see Fig. 1). Most electrons (trapped electrons) are confined in the plasma by the space charge potential well $-e\Phi$, with e the elementary charge and Φ the ambipolar potential. Only the most energetic electrons with a total energy ε larger than the potential energy at the wall $-e\Phi_w$ (free electrons) are capable to overcome this potential barrier and reach the wall. During the afterglow that is accompanied by a collapse of the ambipolar potential, the EDF is always depleted of the most energetic electrons, the free electrons, leading to a rapid cooling of the EDF. In his experiments, Biondi determined the ''electron temperature'' through the ambipolar diffusion coefficient obtained from measurements of the plasma density decay. He showed that in certain cases diffusive cooling can lead to ''electron temperatures'' as low as 30 °K whereas the gas temperature was 300 °K. The reason that electrons can be subcooled to ''temperatures'' below the gas temperature is that in the late afterglow of the discharge, elastic electron-atom collisions are the only electron heating mechanism remaining. If the thermal contact between the gas atoms and the electrons is poor due to low gas pressure and/or heavy gas atoms the diffusive cooling maybe more efficient than collisional heating. (Remember that the average energy transfer in elastic collisions scales with the ratio of the electron to atom mass.)

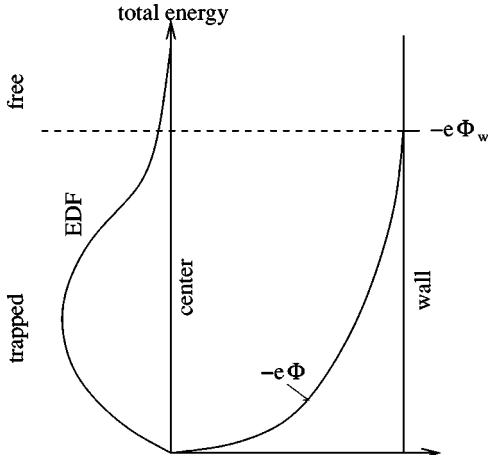

FIG. 1. Schematic of ''diffusive cooling.'' Most of the electrons are trapped by the ambipolar potential well $-e\Phi$. Only free electrons with a total energy larger than the wall potential energy $-e\Phi_w$ are able to reach the wall.

The effect of diffusive cooling has extensively been studied in swarm physics. In swarms, unlike plasmas, electron diffusion can be considered as free diffusion rather than ambipolar. Parker developed the theory of cooling through free diffusion of electrons [13]. Significant effects of diffusive cooling were observed in the swarm experiments reported by Rhymes and Crompton [14]. More recently, diffusion cooling of swarms has been considered in the presence of magnetic fields [15].

The effect of ambipolar diffusive cooling in plasmas is contained in a number of models [5,16,17] in the sense that the electron loss to the wall was identified as the main energy loss mechanism. However, the detailed effects of diffusive cooling on the EDF were not studied in these models due to the assumption of a Maxwellian distribution. An attempt to model the EDF evolution in the afterglow through solution of the Boltzmann equation was reported by Bräuer *et al.* [18]. In their calculations the authors proposed to account for diffusion by using a general diffusion loss term in the Boltzmann equation that had the same magnitude at all energies. However, the model gave only poor agreement with accompanying measurements suggesting the presence of some fundamental deficiencies. In particular, the authors did not distinguish between trapped and free electrons as already suggested by Biondi [12].

More recently a more detailed kinetic approach was proposed by Arslanbekov and co-workers [19,20] based on Biondi's idea of confinement of trapped electrons and the loss of free electrons. The authors identify two main mechanisms for loss of electrons and of electron energy:

(1) Since the EDF is depleted of energetic electrons, the sheath potential starts to collapse. The physical reason for this is that the removal of energetic electrons leads to a slight reduction of the electron flux leaving the plasma. This causes a slight imbalance of electron and ion flux and leads to a reduction of the overall positive space charge of the plasma and hence to a reduction of the sheath potential. The fact that the sheath potential decreases corresponds to a lowering of the potential barrier for electrons. This leads to previously trapped electrons being transformed into free electrons that are now able to reach the wall. The authors call this effect the ''cutoff'' effect since the freeing of previously trapped electrons leads to a cutting off of the EDF at the position of the momentary wall potential energy.

(2) Trapped electrons gain energy through electron-electron collisions and are pushed to total energies higher than the wall potential energy. They become free electrons and can escape to the wall. This mechanism would occur even if the potential in the plasma would not change.

While a number of experimental investigations have studied the EDF evolution in afterglow plasmas, to our knowledge, the effect of diffusive cooling on the EDF has not been demonstrated. A number of studies were performed at pressures that were too high to display pronounced diffusive cooling [21,22]. Based on the results of our studies presented below, we believe that diffusive cooling can, in fact, be found in the EDFs measured in Ref. [18]; however, it was not recognized as such in that work. Hence the objective of this paper is a systematic experimental studied with the aim to demonstrate the effect of diffusive cooling on measured EDFs in the afterglow of a pulsed low-pressure plasma. In addition, we present a very simple semianalytical model based on the idea of the EDF cutoff mechanism that qualitatively reproduces our experimental results.

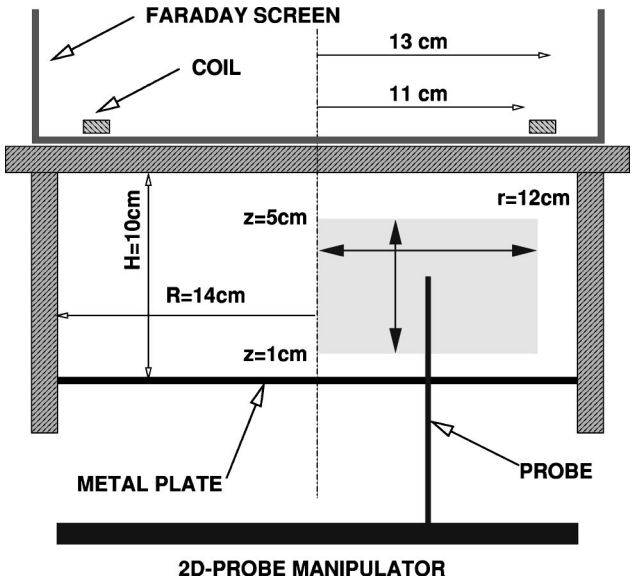

FIG. 2. Schematic of the experimental setup.

This paper is organized as follows. A brief description of the experimental setup is presented in Sec. II. Experimental results are presented and discussed in Sec. III. A simple model is presented in Sec. VI and compared to experimental results. Conclusions are presented in Sec. V.

II. EXPERIMENTAL SETUP

A schematic of the experimental setup is given in Fig. 2. The measurements have been performed in an inductively coupled plasma (ICP) that is sustained in a Pyrex glass chamber with an inner diameter of 28 cm and a height of 10 cm. On the top, the chamber is bound by a flat 1.9-cm-thick Pyrex plate. A hole patterned, grounded sheet metal plate forms the lower boundary of the plasma. It also serves as the reference electrode for the probe measurements. The hole pattern allows gas inlet and pumping with a 1000-l/s turbo pump. The gas pressure was changed between 5 and 70 mTorr (0.66–9.3 Pa). Argon gas was used for all studies presented below. The plasma was produced by a flat one-turn induction coil situated above the top Pyrex plate with an inner radius of 11 cm and an outer radius of 13 cm. The coil is Faraday shielded to eliminate electrostatic coupling to the plasmas.

The studies of the EDF in the afterglow plasma were performed using a Langmuir probe with 5 mm length and 0.254 mm diameter. The probe was introduced into the discharge through a radial slit in the bottom plate. A two-dimensional probe manipulator allowed movement of the probe in radial and axial directions. However, for all measurements presented here the probe was positioned in the discharge center. The probe bias voltage was provided by a Kepco BOP 100-1m voltage amplifier that was driven by the digital-to-

analog output of a National Instruments PCI-6110E data acquisition card. The probe current was measured through the voltage drop over a 10-Ω resistor. This voltage was electrically isolated from ground through a LeCroy 1850A differential amplifier. The voltage drop, which is proportional to the probe current, was measured with the data acquisition card. The card provides 12-bit resolution and allows sampling frequencies of up to 5×10^6 samples/sec.

The plasma was pulsed at a modulation frequency of 1 kHz and a 50% duty cycle. The probe voltage was swept in a range from -17V to $+17$V at a frequency of 0.02 Hz. The probe voltage thus changed only very slightly over many afterglow cycles. During each afterglow cycle the wave form of the probe current $I_{p,V=\mathrm{const}}(t)$ was recorded for the first 100 μs with the AD-converter card at a sampling frequency of 2 MHz. The wave forms of 10 successive afterglows were averaged and associated with the probe voltage at the middle of this ten sample interval. After a complete sweep of the probe voltage range, the measured current wave forms at constant probe voltage $I_{p,V=\mathrm{const}}(t)$ were cross converted into a complete time sequence of I-V probe characteristics $I_{p,t=\mathrm{const}}(V)$ at constant times in the afterglow. In order to improve the signal-to-noise ratio, 400 sweeps of the probe voltage were performed and the resulting I-V characteristics averaged. To record a complete sequence of probe characteristics $I_{p,t=\mathrm{const}}(V)$ for times between 0.5 to 100 μs with 0.5-μs resolution thus took about 5 h.

The EDFs were determined using the well-known Druyvesteyn method [23]. The second derivatives of the probe characteristic required by this method were obtained using a modified Savitzy-Golay smoothing filter [24]. The apparatus function of the filter was dynamically adjusted through the width of the interval used to process the data so that the width of the apparatus function was always less than 2/3 of the observed electron ''temperature'' defined as 2/3 of the mean kinetic energy. In order to improve the dynamic range of the EDFs in the high energy part we also subtracted the contribution due to the ion current curvature. For this purpose, we assumed that the ion current can be approximated as $I_i\propto\sqrt{V_{pl}-V}$, where V_{pl} is the plasma potential defined by the crossover of the second derivative of the probe characteristic. This relation was fitted to the probe characteristics in the ion saturation range where the electron current is negligible.

III. EXPERIMENTAL RESULTS AND DISCUSSION

In the following we will present probe measurements of the EDF evolution in the afterglow plasma. Figure 3 shows the decay of the EDF in the first 30 μs into the afterglow for two different gas pressures of 15 mTorr and 70 mTorr. The EDF at 1 μs into the afterglow at 15 mTorr shows the three temperature behavior well known for the steady state ICP plasma at low electron density. The electron density in this case is $n_e=3.8\times10^{10}$ cm^{-3}. The low energy peak is usually attributed to the nonlocality of the EDF enhanced by the Ramsauer effect in Argon. The common wisdom about the drop at high energies is that it is caused by the inset of inelastic collisions. However, as we will discuss in a moment

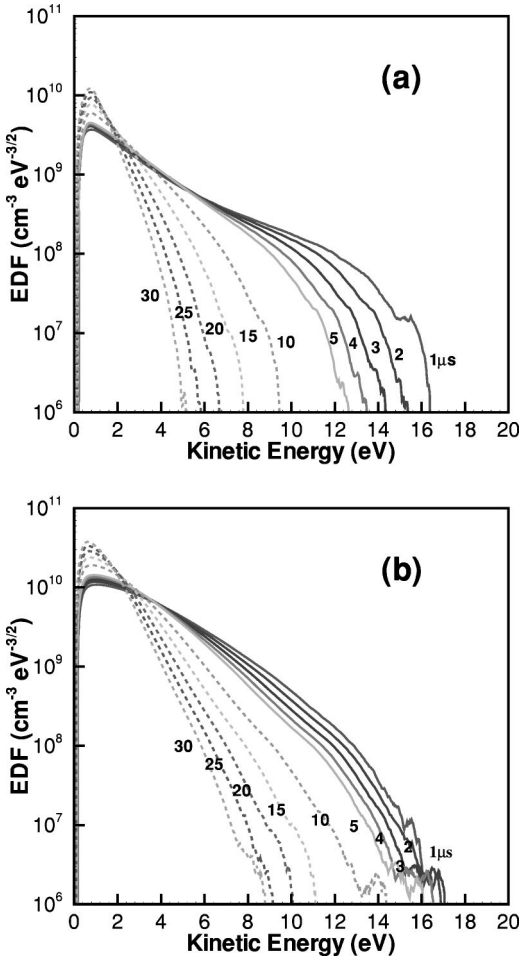

FIG. 3. Measured EDFs in the afterglow at (a) 15 mTorr and (b) 70 mTorr.

this will turn out not to be the main reason in our case. The EDF at 70 mTorr lacks the low energy peak and resembles more a Druyvesteyn distribution. It also shows the drop at high energies.

One indication that the EDF drop at high energies is not related to collisions is that the drop at 70 mTorr is about the same—if not less pronounced—than at 15 mTorr. If the drop were only caused by inelastic collisions, it should be expected that the EDF at 70 mTorr would drop much faster than at 15 mTorr due to the increased frequency of inelastic processes. The idea of inelastic collisions being responsible for relaxation of the EDF high energy range is further invalidated by the observation that the drop of the EDF shifts to lower energies and, for instance, at 10 μs and 15 mTorr appears at around 8 eV. At this energy, however, inelastic collisions are not possible since the inelastic threshold energy in Argon is at 11.55 eV. It can thus be suspected that the drop of the EDF at high energies is a result of electron escape to the wall. Before we discuss this supposition in more detail, we present further evidence that rules out collisions as an important energy loss mechanism.

The observation of the decay of the mean kinetic energy in Fig. 4(a) and the plasma potential in Fig. 4(b) clearly show a behavior incompatible with collisional electron energy re-

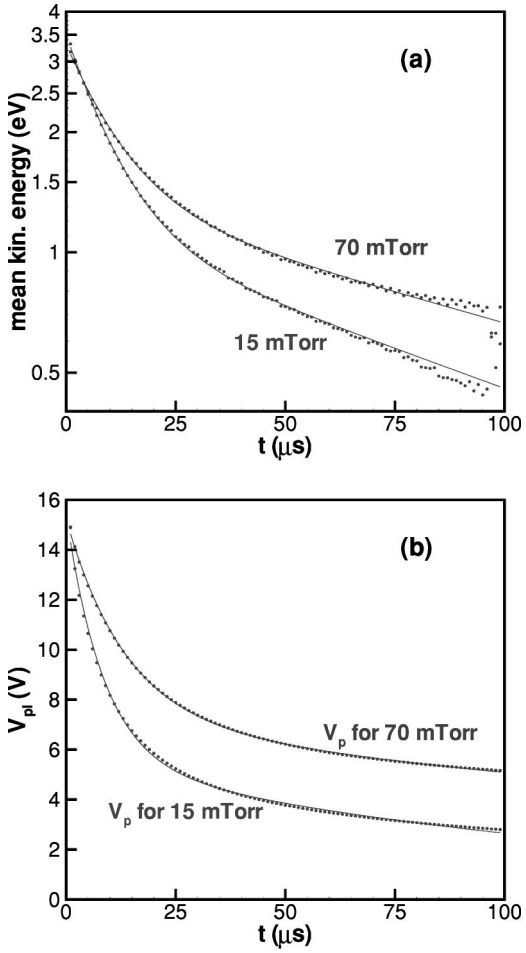

FIG. 4. Decay of the mean kinetic energy (a) and the plasma potential (b) in the afterglow at 15 mTorr and 70 mTorr.

laxation. Unlikely to be expected for collisional energy loss, the energy relaxation at 15 mTorr is even faster than at 70 mTorr. The same holds for the decay of the ambipolar plasma potential.

At all pressures, the temperature decay shows an initial fast decay with a subsequent slower decay. In Fig. 4(a) we have approximated this behavior by a biexponential plot with a fast decay time τ_1 and a slower decay time τ_2. It is instructive to study the dependence of these decay times on the gas pressure, presented in Fig. 5. For all pressures considered, the fast decay time τ_1 is approximately constant while the slower decay time τ_2 increases with pressure. Again, this behavior strongly contradicts collisional energy dissipation as the main energy loss mechanism. A rough comparison of measured decay times and estimate collisional decay times is presented in Table I. The decay time for elastic collisions was estimated for 5-eV electrons, the one for inelastic collisions was estimated for 20-eV electrons. The later decay time is only given for illustration purposes. It is representative for the energy relaxation of the high energy population of the EDF but not identical to an energy decay time for the entire electron population, since the high energy portion of the EDF represents only a small fraction of that. It is more reasonable to compare the measured decay times with the

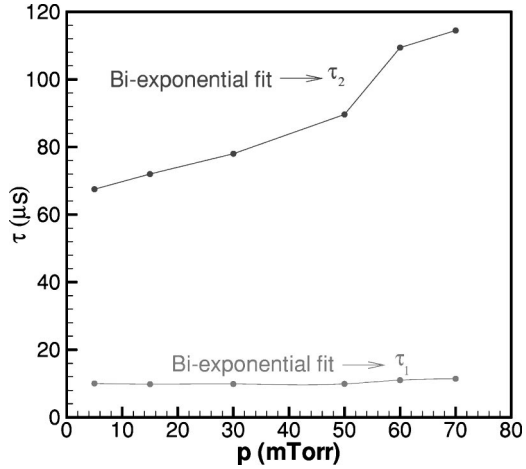

FIG. 5. Measured fast decay times τ_1 and slow decay times τ_2 of the biexponential fits of the electron mean energy decay.

energy relaxation through elastic collisions, which takes over once the high energy part of the EDF is depopulated. Obviously, elastic collisions cannot play an important role at the pressures considered, since their relaxation time is up to two orders of magnitude larger than the observed ones.

In the following we want to relate the observed EDF behavior to the wall loss of electrons. Arslanbekov and coworkers [19,20] have demonstrated that the wall loss of electrons should lead to a distinct drop in the EDF at a total energy that equals the potential energy at the wall $-e\Phi_w$. An explanation for this can be found in the ''nonlocality'' of the EDF in low-pressure discharges [25,26]. When the pressure in a discharge is sufficiently low the collisional energy relaxation becomes inefficient and the typical scale length for electron energy relaxation becomes larger than the discharge dimensions. Under these conditions, the total energy is (in good approximation) a constant of motion and the EDF can be described as a spatially uniform function of total energy (for detailed discussions of the so called nonlocal electron kinetics see [27–29]). Electrons with a total energy below the potential energy at the wall are trapped in the plasma and not able to escape to the wall. The free electron population is subject to a constant drain of electrons leading to the sharp EDF drop in the free electron energy range.

The difference between trapped and free electron regime can clearly be seen in our measurements. In order to demonstrate that the wall potential energy plays a decisive role in the cutoff of the EDF, we plot our measured EDFs against the probe voltage scale instead of energy in Fig. 6. (In fact, this corresponds to plotting of the original second derivatives

TABLE I. Comparison of measured temperature decay times and decay times due to inelastic and elastic collisions.

p (mTorr)	τ_1 (μs)	τ_2 (μs)	τ_{inel} (μs)	τ_{elast} (μs)
5	10	67	0.3	6000
15	10	72	0.1	2000
50	10	88	0.03	600
70	12	114	0.02	430

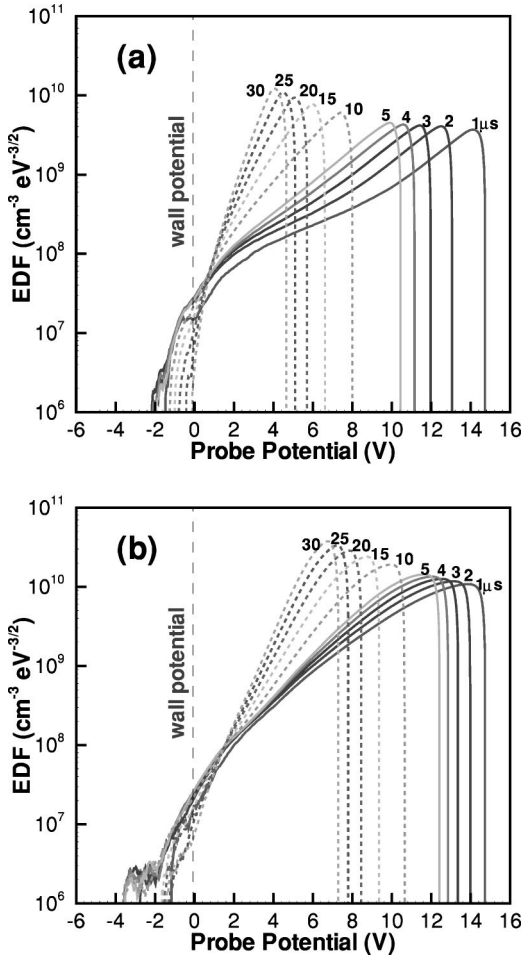

FIG. 6. Measured second derivatives of the probe characteristic at (a) 15 mTorr and (b) 70 mTorr.

of the probe characteristic.) This representation is convenient since one of our walls—the metallic plate—is on ground potential and defines 0 V of our probe voltage scale. As is well-known, the plasma potential at the probe position is given by the crossover of the second derivative, i.e., the steep drop at the right hand side of the curves. The electron energy increases from 0 eV at this probe voltage towards the left, i.e., towards more negative probe voltages. The part of the EDFs between the plasma potential and the wall potential at 0 V represents the trapped electrons, while the part of the curve at negative voltages represents the free electrons. It is clearly seen that the wall potential at 0 V is the point at which the slope of the EDF changes significantly. The steeper drop towards negative probe voltages is representative of the fast loss of free electrons from the discharge. To our knowledge, our measurements are the first to explicitly confirm the effect of electron wall loss on the EDF in afterglow plasmas.

The steeper drop of the free electron part of the EDF at 15 mTorr compared to 70 mTorr is, in fact, also plausible if the electron mean free paths are considered. At 15 mTorr the typical momentum transfer mean free path is about 4 cm. Since the half height of our discharge chamber is 5 cm a considerable number of electrons can reach the wall in free flight. At 70 mTorr, the momentum transfer mean free path is less than 1 cm and the electrons reach the walls only after multiple collisions in a diffusive motion. However, one should keep in mind that the overall loss rate of electrons to the walls is determined by the ion transport rather than by the electrons. After all, for every electron reaching the wall one ion has to be removed from the plasma. In fact, slightly more ions than electrons have to leave the discharge in order to dissipate the positive space charge that creates the ambipolar potential. An increase in pressure hence leads to a slow down in the ion transport which in turn leads to a reduction of the electron wall loss. This is the reason for the increase of the slow decay time τ_2 in Fig. 5 with pressure. At higher pressure, when collisional energy relaxation becomes more important, this trend should, of course, reverse and the energy decay time τ_2 should start to decrease again. The transition pressure between wall loss and collisional energy loss is given by the equality of the ambipolar diffusion frequency and the energy relaxation frequency in elastic collisions:

$$\frac{D_a}{\Lambda^2} = \frac{2m_e}{M_a}\nu_{el}. \tag{1}$$

We expect that at higher pressures of around 300 mTorr for our experiment, the wall loss of electrons will become slower than collisional energy relaxation. In this case the energy relaxation time τ_2 should start to decrease again on further increase of the pressure. Unfortunately, due to the pumping arrangement of our experiment, we are currently not able to test this hypothesis but we expect to do so in the near future.

It should be mentioned that at later times in the afterglow, the measured second derivatives drop into the noise level even at slightly positive voltages. We currently do not have a definitive explanation for this effect. It could possibly be related to asymmetries between our grounded, metallic wall, and the nonconducting walls or to errors in subtracting the ion current.

IV. MODEL

In this section we present a simple model based on the following simple ideas (see Fig. 7):

(1) We assume that the distribution function can be approximated by a Maxwellian distribution that is cut at energies larger than the wall potential energy $-e\Phi_w$.

(2) We assume that when the wall potential decreases, a group of electrons is transformed from trapped into free electrons and lost to the wall immediately (shaded region of the EDF in Fig. 7).

(3) The amount of electrons released through this cutting has to exactly balance the amount of ions lost to the walls. This dependence will be used to define the temporal decay of the plasma potential.

(4) We assume that every electron that is lost to the wall removes an energy equal to the momentary wall potential energy $-e\Phi_w$ from the EDF. This relation will define the decay of the mean energy of the distribution.

As mentioned above, in low-pressure discharges it is

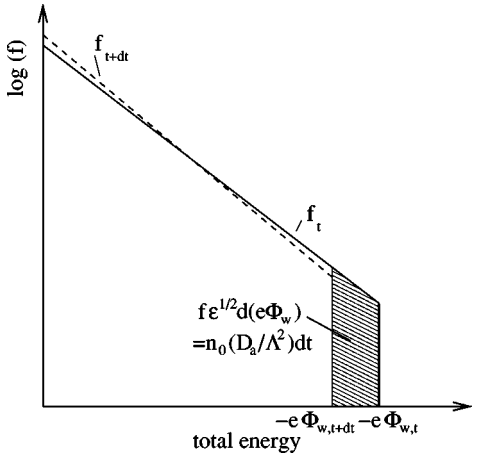

FIG. 7. Scheme of the EDF cutoff mechanism for one time step dt. The electrons in the shaded area of the EDF are released and removed from the discharge through the decay of the wall potential Φ_w. The drop of the plasma potential is determined by the requirement that the electron loss has to be equal to the ambipolar loss of ions. Since the loss of energetic electrons causes an energy loss of the EDF, the slope of the EDF becomes steeper at $t+dt$.

physically reasonable to consider the electron distribution function as a spatially uniform function of the total electron energy ε. We consider the EDF normalized to the electron density in the center,

$$n_0(t)=A\int_0^{-e\Phi_w(t)}\sqrt{\varepsilon'}\exp\left(\frac{-\varepsilon'}{k_bT_e}\right)d\varepsilon'. \tag{2}$$

The integral has to be extended only up to $-e\Phi_w$ since the EDF is considered to be zero above that energy. Here A is a normalization constant, k_b is the Boltzmann constant, and T_e the electron temperature. It is important to note that T_e is merely a parameter describing the slope of the EDF. It is not equal to 2/3 of the mean kinetic energy, since the distribution function is missing the high energy tail at energies above $-e\Phi_w$.

The EDF is represented as

$$f_0(\varepsilon,t)=\begin{cases}\dfrac{n_0(t)\exp(-\varepsilon/k_bT_e)}{\displaystyle\int_0^{-e\Phi_w(t)}\sqrt{\varepsilon'}\exp(-\varepsilon'/k_bT_e)d\varepsilon'} & \text{for } \varepsilon\leqslant-e\Phi_w\\ 0 & \text{for } \varepsilon>-e\Phi_w.\end{cases} \tag{3}$$

When the plasma potential collapses in the afterglow, electrons are ''freed'' and the electron density drops according to the relation

$$\frac{dn_0}{dt}=[\sqrt{\varepsilon}f_0(\varepsilon)]\big|_{\varepsilon=-e\Phi_w}\frac{d(-e\Phi_w)}{dt}. \tag{4}$$

This drop in electron density has to be balanced by an equal drop in ion density that can be written as

$$\frac{dn_0}{dt}=-\frac{n_0}{\tau_{amb}}=-n_0\frac{\Lambda^2}{D_a}. \tag{5}$$

Here D_a is the ambipolar diffusion coefficient $D_a=D_i(1+T_e/T_i)$, with D_i the ion diffusion coefficient, T_e and T_i the electron and ion temperatures, respectively. Λ is the diffusion length diffusion length. Following Ingold [30] we calculate Λ such that the gradient of the assumed axial density profile $n(z)=n_0\cos(x/\Lambda)$ produces a diffusion flux $\Gamma_i=-D_a\nabla n|_s$ at the sheath boundary that matches the Bohm flux $n_s(k_bT_e/M_i)^{1/2}$. The subscript s indicates the density and gradient at the boundary of the sheath that is assumed to be of negligible thickness. This consideration leads to the following transcendental equations for Λ:

$$\tan\left(\frac{L}{2\Lambda}\right)=\sqrt{\frac{k_bT_e}{M_i}}\frac{\Lambda}{D_a}. \tag{6}$$

Here L refers to the full height of the discharge.

With Λ determined from Eq. (6) one can combine Eqs. (3)–(5) to obtain an equation that describes the decay of the wall potential

$$\frac{d(-e\Phi_w)}{dt}=-\frac{\displaystyle\int_0^{-e\Phi_w(t)}\sqrt{\varepsilon'}\exp\left(\frac{-\varepsilon'}{k_bT_e}\right)d\varepsilon'}{\tau_{amb}\sqrt{-e\Phi_w}\exp\left(\dfrac{e\Phi_w}{k_bT_e}\right)}. \tag{7}$$

To determine the change of mean energy over time, the energy balance for trapped electrons has to be considered,

$$\frac{d\langle\varepsilon\rangle}{dt}=-\frac{e\varphi_w}{\tau_{amb}}, \tag{8}$$

where the average electron energy $\langle\varepsilon\rangle$ is a function of the electron temperature T_e and plasma potential:

$$\langle\varepsilon\rangle=\frac{\displaystyle\int_0^{-e\Phi_w}\varepsilon'^{3/2}\exp\left(\frac{-\varepsilon'}{T_e}\right)d\varepsilon'}{\displaystyle\int_0^{-e\Phi_w}\sqrt{\varepsilon'}\exp\left(\frac{-\varepsilon'}{T_e}\right)d\varepsilon'}. \tag{9}$$

The two coupled differential equations (7) and (8) are solved using a Runge-Kutta method. Equation (9) defines the change of the electron temperature T_e and is also solved within our scheme after every Runge-Kutta time step. As initial values in all calculations, we use a wall potential $-\Phi_w=16$ V and a mean kinetic energy as extrapolated to $t=0$ from our experimental values.

Results of our model are represented in Fig. 8. Obviously, the model predicts the decay of the plasma potential rather well, Fig. 8(a). The model shows the same initial rapid decrease of the plasma potential followed by a slower decay as seen in the measurements. Based on the idea of EDF cutting as shown in Fig. 7, the initial fast decay is related to the fact

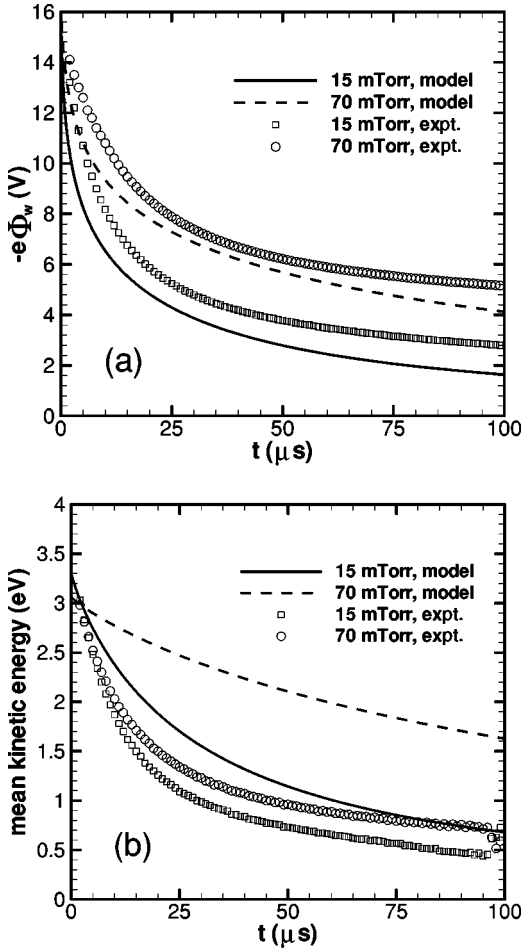

FIG. 8. Measured and calculated decay of the wall potential (a) and mean kinetic energy for 15 mTorr and 70 mTorr.

that initially the high energy part of the EDF is cutoff that contains only few electrons. In order to balance the ion flux, a rather fast initial decrease of Φ_w is required. Unfortunately, the prediction of the decay of the mean kinetic energy is less favorable, Fig. 8(b). While our model reproduces the qualitative trend of a slower decay of the mean energy with increasing pressure, the quantitative comparison, in particular, at 70 mTorr is not very good. Obviously, a more detailed kinetic model would be required to improve the quantitative agreement.

It turns out that the model proposed above, even though founded on the rather different idea of EDF cutting, is almost equivalent to the model proposed by Ashida and Lieberman [5,16]. The energy equation given by these authors is

$$\frac{3}{2}\frac{d}{dt}T_e = -\left[\frac{T_e}{2}\ln\left(\frac{M_i}{2\pi m_e}\right)+T_e\right]\nu_{loss} \qquad (10)$$

with ν_{loss} the loss frequency. This equation is essentially identical to our Eq. (8), if we assume that in our model $\langle\varepsilon\rangle \approx (3/2)T_e$, which is approximately true even for the cut EDF we use in our model. That the right hand sides of Eq. (8) and (10) are mostly equivalent can be seen from the well-known approximation for the potential difference between plasma center and the wall

$$-e\Phi_w = \frac{k_b T_e}{2}\ln\left(\frac{M_i}{2\pi m_e}\right)+T_e\ln\left(\frac{n_0}{n_b}\right), \qquad (11)$$

in which the first term is the potential drop in the sheath and the second term is the potential drop between the center and the sheath boundary in the ambipolar plasma. Since for low-pressure plasmas the logarithm in the second term is close to one, the right hand side of Ashida's and Lieberman's equation is close to $-e\Phi_w\nu_{loss}$ that is identical to the right hand side in our Eq. (8).

V. CONCLUSIONS

In this paper, we have presented measurements performed in the afterglow of the pulsed plasma. The measurements clearly confirm that the wall loss of electrons is the main energy loss mechanism for the EDF. The wall loss of electrons produces a distinct steep drop of the EDF at electron energies higher than the wall potential energy. The fact that free, energetic electrons are constantly lost from the ambipolar potential well while ''cold'' trapped electrons remain confined leads to diffusive cooling of the EDF. In fact, as pointed out by Biondi in 1954, this effect can have the intriguing consequence of being able to produce subcooled electrons at an ''electron temperature'' less than the gas temperature. Unfortunately, the resolution of our probe method is currently insufficient to show such low temperatures as reported by Biondi.

The simple model presented based on the idea of cutting the EDF reproduces the qualitative trends seen in the experiments. The decay of the plasma potential is reproduced rather well while poor quantitative agreement is found with respect to the decay of the electron mean energy. The model is basically equivalent to the model presented previously by Ashida and Lieberman but founded on rather different ideas.

Based on the results presented here, we conclude that the correct distinction between trapped and free electrons is essential for a physically correct description of the EDF evolution in the afterglow of low-pressure plasmas. The lack of this distinction in the theoretical study in Ref. [18] is likely at the basis for the poor agreement between calculated and measured EDFs in that study.

ACKNOWLEDGMENTS

This work was supported in part by the National Science Foundation (Grant No. ECS-9713137), the Department of Energy (Grant No. ER54554), and by the University of Minnesota Supercomputing Institute.

[1] S. Samukawa and S. Furuoya, Appl. Phys. Lett. **63**, 2044 (1993).
[2] S. Samukawa and T. Mieno, Plasma Sources Sci. Technol. **5**, 132 (1996).
[3] J.T. Verdeyen, J. Beberman, and L. Overzet, J. Vac. Sci. Technol. A **8**, 1851 (1990).
[4] A.A. Howling, L. Sansonnens, J.-L. Dorier, and C. Hollenstein, J. Appl. Phys. **75**, 1340 (1994).
[5] S. Ashida, M.R. Shim, and M.A. Lieberman, J. Vac. Sci. Technol. A **14**, 391 (1996).
[6] L.D. Tsendin and Y.B. Golubovskii, Zh. Tekh. Fiz. **47**, 1839 (1977) [Sov. Phys. Tech. Phys. **22**, 1066 (1977)].
[7] R. Winkler, H. Deutsch, J. Wilhelm, and C. Wilke, Beitr. Plasmaphys. **24**, 285 (1984).
[8] R. Winkler, H. Deutsch, J. Wilhelm, and C. Wilke, Beitr. Plasmaphys. **24**, 303 (1984).
[9] P.J. Drallos and J.M. Wadehra, Phys. Rev. A **40**, 1967 (1989).
[10] J. Loureiro, Phys. Rev. E **47**, 1262 (1993).
[11] R. Winkler, M. Dilonardo, M. Capitelli, and J. Wilhelm, Plasma Chem. Plasma Process. **7**, 125 (1987).
[12] M.A. Biondi, Phys. Rev. **93**, 1136 (1954).
[13] J.J.H. Parker, Phys. Rev. **139**, 1792 (1965).
[14] T. Rhymes and R.W. Crompton, Aust. J. Phys. **28**, 675 (1975).
[15] R.E. Robson, Phys. Rev. E **61**, 848 (2000).
[16] S. Ashida, C. Lee, and M. Lieberman, J. Vac. Sci. Technol. A **13**, 2498 (1995).
[17] V. Kolobov, L.D. Lymberopoulos, and D.J. Economou, Phys. Rev. E **55**, 3408 (1997).
[18] T. Bräuer *et al.*, J. Phys. D **30**, 3223 (1997).
[19] R.R. Arslanbekov and A.A. Kudryavtsev, Phys. Rev. E **58**, 7785 (1998).
[20] R.R. Arslanbekov, A.A. Kudryavtsev, and L.D. Tsendin, Phys. Rev. E **64**, 016401 (2001).
[21] L. Overzet and J. Kleber, Plasma Sources Sci. Technol. **7**, 512 (1998).
[22] R. Hugon, G. Henrion, and M. Fabry, Meas. Sci. Technol. **7**, 553 (1996).
[23] M.J. Druyvesteyn, Z. Phys. **64**, 781 (1930).
[24] J.I.F. Palop, J. Ballesteros, V. Colomer, and H.A. Hernández, Rev. Sci. Instrum. **66**, 4625 (1995).
[25] I.B. Bernstein and T. Holstein, Phys. Rev. **94**, 1475 (1954).
[26] L.D. Tsendin, Zh. Eksp. Teor. Fiz. **66**, 1638 (1974) [Sov. Phys. JETP **39**, 805 (1974)].
[27] L.D. Tsendin, Plasma Sources Sci. Technol. **4**, 200 (1995).
[28] U. Kortshagen, C. Busch, and L.D. Tsendin, Plasma Sources Sci. Technol. **5**, 1 (1996).
[29] V. Kolobov and W.N.G. Hitchon, Phys. Rev. E **52**, 972 (1995).
[30] J. H. Ingold, in *Gaseous Electronics*, edited by M. N. Hirsh and H. J. Oskam (Academic Press, New York, 1978).